Research Square

Preprints are preliminary reports that have not undergone peer review.
They should not be considered conclusive, used to inform clinical practice,
or referenced by the media as validated information.

Graphene Oxide Accelerate Diabetic Wound Repair by Inhibiting Apoptosis of Ad-MSCs via Linc00324/miR-7977/STK4 Pathway

Zhe Ji
Xuzhou Medical College Affiliated Hospital
Feifei Chen
Xuzhou Medical University
Shuai Yang
Xuzhou Medical College Affiliated Hospital
Caiqi Shen
Xuzhou Medical College Affiliated Hospital
Hanxiao Wei
Xuzhou Medical College Affiliated Hospital
Qiang Li
Xuzhou Medical College Affiliated Hospital
Peisheng Jin (100000401006@xzhmu.edu.cn)
Xuzhou Medical College Affiliated Hospital https://orcid.org/0000-0002-2239-0156

Research

Keywords: Diabetic wound, Graphene Oxide, adipose-derived mesenchymal stem cells, Linc00324, miR-7977

Posted Date: March 22nd, 2021

DOI: https://doi.org/10.21203/rs.3.rs-336416/v1

License: This work is licensed under a Creative Commons Attribution 4.0 International License.
Read Full License

Abstract

Background

Graphene oxide (GO) has been proven in many studies to promote the proliferation and differentiation of a variety of stem cells, but its effect on the apoptosis of adipose-derived mesenchymal stem cells (Ad-MSCs) is still unclear. Apoptosis is one of the most important factors in the treatment of diabetic wounds by stem cells. Therefore, we explored its therapeutic effect on diabetic wounds by studying the effect of GO on the apoptosis of Ad-MSCs.

Methods

qRT-PCR was used to detect the expression of lncRNAs, miRNAs and mRNAs in Ad-MSCs. RNA immunoprecipitation (RIP), RNA pull-down and luciferase assays were used to detect the interaction of the specific lncRNA, miRNA and mRNA. The effects of Linc00324 on Ad-MSCs cells apoptosis were explored by flow cytometer, TUNEL assay and Western blot. Diabetic wound was established to explore the function of Linc00324 on Ad-MSCs repairing ability in vivo.

Results

GO inhibited the apoptosis of Ad-MSCs caused by high glucose, and Linc00324 was one of the factors contributing to its effect. In terms of mechanism, RIP and RNA-Pull-down confirmed Linc00324 could directly interact with miR-7977, and then acted as a miRNA sponge to regulate the expression of miR-7977 target gene STK4 (MST1) and downstream signaling pathways. In addition, GO reduced the apoptosis of Ad-MSCs in wounds and promoted wound healing.

Conclusions

Overall, this study highlights that GO maybe a superior auxiliary material for Ad-MSCs to repair diabetic wounds via Linc00324/miR-7977/STK4 pathway.

Introduction

The formation of chronic diabetic wounds is related to many factors [1, 2]. In the human body, stem cells play an important role in wound repair[3]. At present, a variety of stem cells including Ad-MSCs have been used to treat diabetic wounds[4–6]. After the body is damaged, Ad-MSCs in the body can mobilize and chemoattract to the injured site, play the role of wound repair[7]. However, in a high glucose environment, the apoptosis of Ad-MSCs increases, which weakens the ability to repair wounds[8].

GO,an important derivative of graphene[9], has been widely used in biomedical fields such as disease detection[10], regenerative medicine[11, 12]. Studies have shown that GO-related materials have antibacterial effects [13, 14], which makes it promising to be used in the field of wound healing. Studies shown that GO promoted the differentiation of stem cell[15–17]and had effects on structure for the

adhesion, proliferation of human adipose-derived stem cells[18]. but its effect on cell apoptosis has not been studied yet. Therefore, we designed relevant experiments to study the role of GO in cell apoptosis and diabetic wound healing.

The RNA between genes longer than 200bp and does not encode protein is called large non-coding RNA (LncRNA)[19]. LncRNA has been identified and clearly proved its role in cell proliferation, apoptosis, invasion. Among them, Linc00324 has been proved to be related to cell proliferation, invasion and migration in many studies[20, 21], but its role in cell apoptosis is not clear. miRNA is a type of non-coding RNA with a length of 19–24 nt that exists in eukaryotes[22]. In recent studies, LncRNA has been shown to act as competing endogenous RNAs (ceRNAs) to bind miRNAs[23]. For example, Linc00324 acts as a ceRNA to promote proliferation, migration and invasion of colorectal cancer cell via targeting miR-214-3p[21]. MEG3 acts as a ceRNA to regulate ischemic neuronal death by targeting the miR-21/PDCD4 signaling pathway[24]. However, there is no research report on the role and mechanism of Linc00324 in Ad-MSCs.

In our present study, we observed that Ad-MSCs apoptosis increased in a high-glucose environment; GO decreased cell apoptosis in a high-glucose environment via Linc00324. Linc00324 decoyed miR-7977 as a sponge RNA and regulated the apoptosis of Ad-MSCs through the miR-7977/STK4 axis. Thus, GO promoted the healing of diabetic wounds by reducing cell apoptosis and was a new way to treat diabetic wounds.

Materials And Methods

Cell co-culture

Using Graphene Oxide(Xian feng,China) solutions with final concentrations of 0.1 mg, 0.2 mg, and 0.4 mg/ml to add to the Ad-MSCs culture medium, culture at 37°C, 5% CO_2, and add 40 mM glucose(Although the results of previous experiments showed that apoptosis was higher at 80 mM glucose concentration, it was too far from the blood glucose threshold of diabetic patients, so we chose 40 mM concentration for in vitro experiments.). After 48 hours of incubation, other experiments were performed.

CM-Dil staining

CM-Dil (Invitrogen, USA) labels cells by binding to lipid molecules of membrane structure, with strong and stable red fluorescence (excitation peak 420nm/emission peak 488nm) detected by Xenogen IVIS200 imaging system (Xenogen Corp.).

Western blot

Separate the cell extracts on SDS-polyacrylamide gel, then transfer the protein to nitrocellulose membrane and incubate with rabbit polyclonal antibodies: anti-STK4, anti-BIM, anti-Bax, anti-BCL-2, anti-AGO2 (1:500, Cell Signaling Technology), and mouse monoclonal antibody: anti-β-actin (1:1000, Cell

Signaling Technology). The immunoreactive protein bands were detected with the Tanon scanning system (Tanon Science & Technology Co., Ltd., Beijing, China).

Flow cytometry

Following treatment, Ad-MSCs were stained with PE Annexin V/7-AAD (BD Roche, USA) at 37°C for 1 h, then detected with flow cytometry, and analyzed cell apoptosis with FlowJo_V10 software.

TUNEL assay

Terminal deoxynucleotidyl transferase-mediated dUTP nick end labeling (TUNEL) assay (in situ cell death detection kit; Roche Diagnostics) was used to determine the apoptosis of Ad-MSC. In short, Ad-MSC was incubated with TdT and fluorescein-labeled dUTP at 37°C for 45 minutes. The percentage of apoptotic cells was then evaluated.

The establishment of lentivirus packaging and stable cell lines

The target plasmid (Obio, China) and virus packaging auxiliary plasmids pMD2.G and pSPAX2 (Obio, China) were co-transfected into 293T cells for virus packaging. The virus supernatant was collected after 48 hours of transfection, and after concentration and purification Infect adipose-derived mesenchymal stem cells. 72 hours after the virus infects the cells, the fluorescence efficiency is high.

RNA-Pull Down experiment

Pierce™ magnetic RNA protein pull-down kit (using Thermo Fisher Scientific, Massachusetts, USA) is used for RNA pull-down assay. Biotin-labeled RNAs Transcript Aid T7 high-yield in vitro transcription kit (Thermo Fisher Scientific) and Pierce RNA 3'end desulfurization biotinylation kit (Thermo Fisher Scientific), and then treated with RNase-free DNase I (Thermo Scientific). The recovered protein was detected by Western blot. The procedure is based on the Western blot protocol previously described according to the manufacturer's instructions and standards.

Establishment of wound model of diabetic nude mice

All procedures were approved by the Animal Care and Use Committee of Xuzhou Medical University (project number: XYFY2016-KL033). After fasting (free drinking water) for 12 hours, weighing her body weight and injecting 2% STZ intraperitoneally at a dose of 150 mg/kg. Serum glucose level greater than 16.7 mmol/L for at least 4 weeks was defined as successfully developed diabetic mice model. After anesthetized, a full thickness skin defect of 1.5 cm diameter was made on the back.

RNA binding protein immunoprecipitation

Use Magna RIP™ RNA Binding Protein Immunopurification Kit (Millipore) for RIP analysis. In short, about 5 x 10^6 MSCs were lysed with RIP lysis buffer. Then incubate rabbit IgG conjugated with anti-AGO2 antibody (Millipore, 03-110) or negative control purified rabbit IgG with RIP buffer containing magnetic beads. The positive control anti-SNRNP70 antibody was used in the RIP procedure. The sample was

incubated with proteinase K and the unprecipitated RNA was separated. Precipitate and purify RNA and perform quantitative PCR to purify and detect the presence of target lncRNA or miRNA.

Fluorescence in Situ Hybridization (FISH)

Genepharma synthesized FITC-labeled probes for detection of Linc00324 and Cy3-labeled probes for detection of miR-7977. The signal of the probe was detected by a fluorescence in situ hybridization kit (Genepharma, Shanghai, China) according to the manufacturer's instructions. Images were recorded digitally using a Lei TCS SP8 laser scanning confocal microscope (Leica Microsystems, Mannheim, Germany).

qRT-PCR

As mentioned above[25], RNA is extracted and prepared for qRT-PCR. According to the manufacturer's protocol, the Prime Script reverse transcriptase kit (Takara, Dalian, China) was used to reverse transcribe total RNA to cDNA. Using SYBR Green chemical reagents, quantitative RT-PCR was carried out by Roche-Light Cycler 96 sequence detector (Roche, Germany). The specific primers are provided Table 1.

Evaluation of wound closure

Before harvesting, the size of the wounded area on each mouse back was measured with a ruler and recorded on parfocal digital photographs taken at Day 0, 7and 14 after injecting PBS as a blank control or Ad-MSCs, Linc00324 overexpression Ad-MSCs, Linc00324 knockdown Ad-MSCs, GO + Ad-MSCs, GO + Linc00324 overexpression Ad-MSCs, GO + Linc00324 knockdown Ad-MSCs. Wound closure rate was measured as follows:

Wound closure index (%) = (1- unhealed wound area/original wound area) ×100%

Statistical analysis

The results shown represent an experiment repeated at least three times. All quantitative data are expressed as average SEM. Statistical analysis was performed using SPSS version 22.0 (SPSS Inc, Chicago, Il). Through one-way analysis of variance (ANOVA), and then perform post-test, compare the differences in multiple groups. The difference between the two groups is determined by the student's t-test. P value < 0.05 is considered statistically significant (*P < 0.05)

Results

GO reduced high glucose induced apoptosis of Ad-MSCs.

We detected the increase in apoptosis of Ad-MSCs in a high glucose environment, which is consistent with our previous results (FigS1-S3)[8].After co-culturing GO with Ad-MSCs, we used flow cytometry to detect the apoptosis of Ad-MSCs, and found that the apoptosis rate was significantly reduced in the same high glucose environment after co-cultivation(Fig.S4 A, B). Then we used the TUNEL kit for apoptosis detection, and obtained Similar results (Fig.S4 C, D). Furthermore, with the increase of GO

concentration, the reduction of apoptotic cells was more obvious. The Western blot experiment results showed that the expression of pro-apoptotic molecules BAX, BIM, and STK4 decreased with the increase of GO, and the expression of anti-apoptotic molecule BCL-2 increased with the increase of GO (Fig.S4E,S5), indicating that GO has inhibition of Ad-MSCs apoptosis in high glucose environment.

GO inhibited the expression of Linc00324 in Ad-MSCs.

As we mentioned, Linc00324 has been proved to be related to cell proliferation, invasion and migration in many studies[20, 21], but its role in cell apoptosis is not clear. So, we selected Linc00324 to explore its role in cell apoptosis. After our research, we found that the expression of Linc00324 in Ad-MSCs decreased after increasing the GO concentration during co-cultivation (Fig. 1A, B). So, we chose to establish a cell line that down-regulated and over-expressed Linc00324((Fig. 1C, D) and verify them, and found that under high glucose conditions, the apoptosis of the down-regulated Linc00324 group was significantly reduced, while the over-expression group had the opposite result (Fig. 1E-H, S6). In order to further verify whether GO regulates cell apoptosis through Linc00324, we used a cell line overexpressing Linc00324 to co-culture with GO and found that cell apoptosis did not decrease (Fig. 1J-M). Therefore, Linc00324 was one of the factors that GO regulated apoptosis.

Linc00324 decoyed miR-7977 as a sponge RNA.

In order to determine the mechanism by which Linc00324 regulates Ad-MSCs apoptosis, we performed qPCR to detect the location of Linc00324. Linc00324 is mainly located in the cytoplasm (Fig. 2A, B), which indicates that it may have the function of competing endogenous RNA and can serve as a molecular sponge for miRNA. A search of the miRDB database revealed the 5 miRNAs with the highest binding scores (Fig. 2C). We designed qPCR primers for these five miRNAs to determine whether they are regulated by Linc00324. It is worth noting that the level of miR-7977 was significantly reduced in the Linc00324 overexpression group, but increased in the Linc00324 knockdown group (Fig. 2D). Subsequently, we used RNA-FISH experiments to locate Linc00324 and miR-7977, and found that miR-7977 is also mainly located in the cytoplasm (Fig. 2E). In addition, we predicted the possible sites of Linc00324 in miR-7977, and constructed wild-type (WT) and mutant (MUT) luciferase reporter genes, including firefly and Renilla luciferase sequences (Fig. 2F). According to the result of luciferase assay, miR-7977 mimic reduced the fluorescence of Linc00324 WT, but had no effect on Linc00324 MUT (Fig. 2G).

The endogenous binding between miR-7977 and Linc00324 has been verified by RIP and verified by qPCR analysis. The results showed that compared with the empty vector (MS2) Linc00324 with a mutation (Linc00324-mut) in the miR-7977 targeting site, the Linc00324 RIP in Ad-MSCs was significantly enriched for miR-7977. The vector and another lncRNA-ATB without a predetermined miR-7977 targeting site vector (Fig. 2H). Using biotin-labeled Linc00324 to pull down the affinity of miR-7977 in vitro further confirmed the endogenous binding between miR-7977 and Linc00324 (Fig. 2I).

It is known that miRNA inhibits translation and degrades mRNA in an AGO2 (Argonaute RISC catalytic component 2) dependent manner by binding to the target. In order to prove whether Linc00324 can bind to miR-7977 in this way, we used an RNA pull-down assay to determine whether Linc00324 binds to AGO2. According to the western blot data, Linc00324 instead of AGO2 combined with the antisense control (Fig. 2J). RIP analysis was also performed to verify the interaction of Linc00324 and miR-7977. The enrichment of Linc00324 in the anti-AGO2 group confirmed the binding between Linc00324 and miR-7977 (Fig. 2K, L). In order to further prove the binding mode of Linc00324 and miR-7977, anti-AGO2 RIP was performed in Ad-MSCs with overexpression of miR-7977. The cells transfected with miR-7977 were specifically enriched with endogenous Linc00324 by AGO2 (Fig. 2M), indicating that miR-7977 may be Linc00324-carrying miRNA. Furthermore, we tested the expression level of Linc00324 in the miR-7977 mimics and inhibitors groups, and found that the expression level of Linc00324 decreased in the miR-7977 mimics group, but increased in the inhibitors group (Fig. 2N). Therefore, Linc00324 acted as a sponge for miR-7977.

miR-7977 targeted STK4 to inhibit the apoptosis of Ad-MSCs.

Since Linc00324 and miR-7977 have a competitive endogenous relationship, Linc00324 has been proven to promote cell apoptosis. It was transferred into miR-7977-mimics and inhibitors in the cells respectively. It was found that the miR-7977-mimics group decreased cell apoptosis under high glucose environment and the miR-7977-inhibitors group increased apoptosis by flow cytometer analysis (Fig. 3A, B) and TUNEL assay (Fig. 3C, D). The WB experiment results showed that the expression of BAX, BIM, and STK4 decreased with the transfection of miR-7977-mimics while the expression of BCL-2 increased (Fig. 3E, F). So, miR-7977 reduced the apoptosis of Ad-MSCs. What is the reason why miR-7977 reduces apoptosis? By predicting the downstream targets of miR-7977 via miRDB MicroRNA Target Prediction (Fig. 4A), we selected STK4, which is also called MST1,closely related to apoptosis[26]. To confirm whether miR-7977 targets STK4, we cloned the 3’UTR sequence of STK4 into the psiCHECK™-2 vector. and constructed a mutant 3'-UTR report that has no binding site to miR-7977(Fig. 4B). The data showed that introduction of miR-7977 diminished luciferase activity of this reporter and the activity of the mutant 3'-UTR reporter gene remained unchanged (Fig. 4C). At the same time, it was verified by qPCR and western blot experiments that miR-7977 had an inhibitory effect on STK4 at mRNA and protein levels (Fig. 4D-F). We added the STK4 inhibitor XMU-MP-1 to the miR-7977 inhibitor group. Flow cytometry analysis showed that XMU-MP-1 inhibited miR-7977 inhibitors apoptosis (Fig. 4G, H), which is consistent with the results of TUNEL analysis (Fig. 4I, J) and Western blot analysis (Fig. 4K, S7). So miR-7977 could directly target the 3’-UTR of STK4 and downregulate STK4 expression and inhibited the apoptosis of Ad-MSCs.

Linc00324 regulated the apoptosis of Ad-MSCs induced by high glucose through miR-7977/STK4.

We further investigated whether the miR-7977/STK4 axis is involved in the regulation of apoptosis by Linc00324 in a high glucose environment. We co-transfected Ad-MSCs with miR-7977 mimics and overexpression Linc00324 and found that miR-7977 mimics can significantly inhibit the apoptosis caused by overexpression Linc00324 via flow cytometry analysis (Fig. 5A, B). The TUNEL assay (Fig. 5C,

D) and Western blot experiment (Fig. 5E, Fig.S8) also got consistent results. In addition, we also used miR-7977 inhibitors and down-regulated Linc00324 to co-transfect Ad-MSCs. The results showed that the miR-7977 inhibitors group reversed the decrease in apoptosis caused by downregulation of Linc00324(Fig. 5F-J, Fig S9). Based on the above data, Linc00324 regulated the apoptosis of Ad-MSCs induced by high glucose through miR-7977/STK4.

GO inhibited cell apoptosis and promoted wound healing in diabetic nude mice.

In order to further prove the effect of GO on Ad-MSCs-mediated wound healing of diabetic nude mice, we simulated and established a wound repair model with human skin wounds in diabetic nude mice. We established a wound with a diameter of 1.5 cm, and injected the treated cells with the fluorescent dye CM-DiI into the skin of the wound margin of each group of nude mice by intradermal injection, and tested the cell survival rate after 7 days It was found that the down-regulated Linc00324 and GO mixed culture group had the highest survival rate(Fig. 6A, B). Then we evaluated the wound healing effect of nude mice for 14 days. The results suggest that the GO group is better than the blank control group, and the down-regulated Linc00324 and GO mixed culture group has the best wound healing effect (Fig. 6C, D). Besides, the HE and Masson staining of tissue sections showed that the best group is still the down-regulation group Linc00324 and GO mixed culture group (Fig. 6E, F). We further used tissue immunofluorescence to detect the angiogenesis (CD31) and inflammation (TNF-α) of the wound tissue, and found that the expression of CD31 was high in the down-regulated group and the GO group, while the expression of TNF-α was low, suggesting good wound healing (Fig. 6G-I). We used the tissue of the wound to perform an ELISA test to detect the cytokines related to wound healing and obtained similar results (Fig. 6J). The results of in vivo experiments suggested that GO could inhibit the apoptosis of stem cells in diabetic nude mice, thereby promoting wound healing.

Discussion

Diabetes wounds are a clinical problem that urgently needs to be solved, and it is also a problem that has plagued clinicians for many years[27–30]. At present, studies have reported that graphene and stem cells have an effect on the repair of skin wounds[31]. Graphene provided protection against microbial invasion and strategies aimed at minimizing the incidence of sepsis, while MSCs can secrete a variety of factors that have therapeutic effects on the repair of skin damage and tissue regeneration [32]. However, there has been no relevant research on treatment of diabetic wounds by GO. Therefore, we used GO to repair wounds, it has antibacterial effects and enhances the repair of seed cells, which is more helpful for the repair of diabetic wounds.

Apoptosis became the reason that the poor treatment of diabetic wounds by stem cells. We found that under high glucose environment, the apoptosis of Ad-MSCs increased (Fig S1-S3). So, we designed to add GO co-cultured with Ad-MSCs and found that GO can reduce the apoptosis of Ad-MSCs under high glucose environment (Fig S4). In order to further explore the principle of this phenomenon, we turned our attention to Lnc RNA, which has been shown to have an effect on cell apoptosis in a number of studies

this year. For example, Lnc IGF2AS regulates human retinal pigment endothelial cell apoptosis induced by high glucose[33]. In diabetic cardiomyopathy, the down-regulation of LncRNA H19 leads to the oxidative response in diabetic rats[34]. These provide us with new ideas for studying the mechanism of GO regulating cell apoptosis. We found that the expression of Linc00324 decreased significantly after co-cultivation. Subsequently, we found that Linc00324 promotes cell apoptosis in a high glucose environment. In order to verify whether Linc00324 is a factor of GO regulating cell apoptosis, we designed to add GO to the Linc00324 overexpression group to co-culture, and found that the anti-apoptotic effect of GO disappeared.

LncRNA has different functions due to different distributions. In order to further explore the mechanism of Linc00324 regulating cell apoptosis, we conducted localization experiments on Linc00324 and found that it is mainly distributed in the cytoplasm, while cytoplasmic LncRNA mainly plays a role through ceRNA. Then through bioinformatics prediction, we found miRNA-miR-7977 that has a binding site with Linc00324. miRNAs interacted with the AGO protein family to suppress translation or degrade mRNA. Then we combined the RIP and RNA-pull-down experiments to prove that Linc00324 can bind to the AGO2 protein. The luciferase reporter assay further verified that Linc00324 can inhibit the expression of miR-7977. qRT-PCR was performed in the miR-7977-inhibitors group and found that Linc00324 was increased. It confirmed that Linc00324 decoyed miR-7977 as a sponge RNA.

miRNA is involved in the regulation of post-transcriptional gene expression in cell biology. In blood diseases, miR-7977 is believed to be transferred to bone marrow mesenchymal stromal cells (MSCs) and reduce the proliferation ability of MSCs stem/progenitor cells by reducing PCBP1 protein, leading to AML and MDS Normal hematopoietic dysfunction[35].Chen found that miR-7977 is closely related to the occurrence and development of lung cancer, and can suppress tumor cell invasion and migration[36]. Since Linc00324 sponged miR-7977 as a ceRNA, we studied role of miR-7977 on Ad-MSCs apoptosis and found that miR-7977 reduced apoptosis.

In order to better elucidate the apoptosis effect of miR-7977 in regulating Ad-MSCs, we predicted and detected the target gene STK4 of miR-7977 through bioinformatics, and through experiments proved that miR-7977 can target STK4 and inhibit it at the transcription and translation level. Its expression. STK4 is a serine/threonine kinase. As a key component of the Hippo signaling pathway, STK4 plays a key role in organ size control and tumor suppression by limiting proliferation and promoting apoptosis[37, 38]. We verified that Linc00324 regulates the apoptosis of Ad-MSCs through miR-7977/STK4, thus elucidating the mechanism which GO can reduce the apoptosis of Ad-MSCs in a high glucose environment. Subsequently, animal experiments verified the role of GO in reducing apoptosis and promoting wound healing. After down-regulating Linc00324, co-cultivation with GO achieved the best repair effect.

Conclusion

In summary, GO reduced the expression of Linc00324, while Linc00324 increased cell apoptosis in a high-glucose environment via miR-7977 as a ceRNA,and regulated STK4 to apoptosis of Ad-MSCs. Therefore,

GO as an emerging biomaterial, is resistant to diabetic wound healing has a good therapeutic prospect and is expected to become a new treatment option.

Abbreviations

Ad-MSCs: adipose-derived mesenchymal stem cells; FISH: Telomere fluorescence in situ hybridization; TUNEL: Terminal deoxynucleotidy1 transferase-mediated dUTP nick end-labeling; LncRNAs: Long non-coding RNAs; miRNA: microRNA; STK4: Serine/threonine-protein kinase 4; HE: hematoxylin and eosin; AGO2: Argonaute RISC catalytic component 2; EGF: Epidermal growth factor; VEGF: Vascular endothelial growth factor; DAPI: 4,6-diamidino-2-phenylindole; qRT-PCR: Quantitative real-time PCR.

Declarations

Acknowledgements

Not applicable.

Author Contributions

PSJ and QL conceived and designed the experiments. ZJ, FFC and SY participated in the experiments and drafted the manuscript. ZJ contributed to the sample collection and interpretation of the data. CQS and HXW performed the statistical analysis. FFC revised the manuscript. All authors read and approved the final manuscript.

Funding

This Project was supported by grants from the National Natural Science Foundation of China (82072819), the National Natural Science Foundation of Jiangsu Province (BK20201155), China Postdoctoral Science Foundation (2019T120462), Jiangsu Postdoctoral Science Foundation (2019K155) and Postgraduate Research & Practice Innovation Program of Jiangsu Province (KYCX20_2456, KYCX20_2480).

Availability of data and materials

The datasets and resources generated during and/or analyzed during the current study are available from the corresponding author upon reasonable request.

Ethics approval and consent to participate

All animal experiments and all protocols were authorized by Guide for Animal Care and Use Committee of Xuzhou Medical University (XYFY2016-KL033).

Consent for publication

Not applicable.

Competing interests

The authors declare no competing financial interests.

References

1. Barman PK, Koh TJ. Macrophage Dysregulation and Impaired Skin Wound Healing in Diabetes. Front Cell Dev Biol 2020;8:528.
2. Dong X, Yang L. Inhibition of fatty acid binding protein 4 attenuates gestational diabetes mellitus. Prostaglandins Leukot Essent Fatty Acids 2020;161:102179.
3. Dekoninck S, Blanpain C. Stem cell dynamics, migration and plasticity during wound healing. Nat Cell Biol 2019;21(1):18-24.
4. Tyeb S, Shiekh PA, Verma V, Kumar A. Adipose-Derived Stem Cells (ADSCs) Loaded Gelatin-Sericin-Laminin Cryogels for Tissue Regeneration in Diabetic Wounds. Biomacromolecules 2020;21(2):294-304.
5. Dhoke NR, Kaushik K, Das A. Cxcr6-Based Mesenchymal Stem Cell Gene Therapy Potentiates Skin Regeneration in Murine Diabetic Wounds. Mol Ther 2020;28(5):1314-1326.
6. Moradi A, Zare F, Mostafavinia A, Safaju S, Shahbazi A, Habibi M, et al. Photobiomodulation plus Adipose-derived Stem Cells Improve Healing of Ischemic Infected Wounds in Type 2 Diabetic Rats. Sci Rep 2020;10(1):1206.
7. Li Q, Guo Y, Chen F, Liu J, Jin P. Stromal cell-derived factor-1 promotes human adipose tissue-derived stem cell survival and chronic wound healing. Exp Ther Med 2016;12(1):45-50.
8. Li Q, Xia S, Yin Y, Guo Y, Chen F, Jin P. miR-5591-5p regulates the effect of ADSCs in repairing diabetic wound via targeting AGEs/AGER/JNK signaling axis. Cell Death Dis 2018;9(5):566.
9. Novoselov KS, Geim AK, Morozov SV, Jiang D, Zhang Y, Dubonos SV, et al. Electric field effect in atomically thin carbon films. Science 2004;306(5696):666-669.
10. Xu S, Liu Y, Wang T, Li J. Positive potential operation of a cathodic electrogenerated chemiluminescence immunosensor based on luminol and graphene for cancer biomarker detection. Anal Chem 2011;83(10):3817-3823.
11. Choe G, Oh S, Seok JM, Park SA, Lee JY. Graphene oxide/alginate composites as novel bioinks for three-dimensional mesenchymal stem cell printing and bone regeneration applications. Nanoscale 2019;11(48):23275-23285.
12. Zambrano-Andazol I, Vazquez N, Chacon M, Sanchez-Avila RM, Persinal M, Blanco C, et al. Reduced graphene oxide membranes in ocular regenerative medicine. Mater Sci Eng C Mater Biol Appl 2020;114:111075.
13. Kim S, Le TH, Park CS, Park G, Kim KH, Kim S, et al. A Solution-Processable, Nanostructured, and Conductive Graphene/Polyaniline Hybrid Coating for Metal-Corrosion Protection and Monitoring. Sci

Rep 2017;7(1):15184.

14. Yousefi M, Dadashpour M, Hejazi M, Hasanzadeh M, Behnam B, de la Guardia M, et al. Anti-bacterial activity of graphene oxide as a new weapon nanomaterial to combat multidrug-resistance bacteria. Mater Sci Eng C Mater Biol Appl 2017;74:568-581.
15. Fu C, Pan S, Ma Y, Kong W, Qi Z, Yang X. Effect of electrical stimulation combined with graphene-oxide-based membranes on neural stem cell proliferation and differentiation. Artif Cells Nanomed Biotechnol 2019;47(1):1867-1876.
16. Kim TH, Lee KB, Choi JW. 3D graphene oxide-encapsulated gold nanoparticles to detect neural stem cell differentiation. Biomaterials 2013;34(34):8660-8670.
17. Garcia-Alegria E, Iliut M, Stefanska M, Silva C, Heeg S, Kimber SJ, et al. Graphene Oxide promotes embryonic stem cell differentiation to haematopoietic lineage. Sci Rep 2016;6:25917.
18. Kim J, Choi KS, Kim Y, Lim KT, Seonwoo H, Park Y, et al. Bioactive effects of graphene oxide cell culture substratum on structure and function of human adipose-derived stem cells. J Biomed Mater Res A 2013;101(12):3520-3530.
19. Ali T, Grote P. Beyond the RNA-dependent function of LncRNA genes. Elife 2020;9.
20. Wu S, Gu Z, Wu Y, Wu W, Mao B, Zhao S. LINC00324 accelerates the proliferation and migration of osteosarcoma through regulating WDR66. J Cell Physiol 2020;235(1):339-348.
21. Ni X, Xie JK, Wang H, Song HR. Knockdown of long non-coding RNA LINC00324 inhibits proliferation, migration and invasion of colorectal cancer cell via targeting miR-214-3p. Eur Rev Med Pharmacol Sci 2019;23(24):10740-10750.
22. Tyc KM, Wong A, Scott RT, Jr., Tao X, Schindler K, Xing J. Analysis of DNA variants in miRNAs and miRNA 3'UTR binding sites in female infertility patients. Lab Invest 2020.
23. Zhu J, Deng J, Zhang L, Zhao J, Zhou F, Liu N, et al. Reconstruction of lncRNA-miRNA-mRNA network based on competitive endogenous RNA reveals functional lncRNAs in skin cutaneous melanoma. BMC Cancer 2020;20(1):927.
24. Yan H, Rao J, Yuan J, Gao L, Huang W, Zhao L, et al. Long non-coding RNA MEG3 functions as a competing endogenous RNA to regulate ischemic neuronal death by targeting miR-21/PDCD4 signaling pathway. Cell Death Dis 2017;8(12):3211.
25. Zhang YX, Yan YF, Liu YM, Li YJ, Zhang HH, Pang M, et al. Smad3-related miRNAs regulated oncogenic TRIB2 promoter activity to effectively suppress lung adenocarcinoma growth. Cell Death Dis 2016;7(12):e2528.
26. Turunen SP, von Nandelstadh P, Ohman T, Gucciardo E, Seashore-Ludlow B, Martins B, et al. FGFR4 phosphorylates MST1 to confer breast cancer cells resistance to MST1/2-dependent apoptosis. Cell Death Differ 2019;26(12):2577-2593.
27. Wear-Maggitti K, Lee J, Conejero A, Schmidt AM, Grant R, Breitbart A. Use of topical sRAGE in diabetic wounds increases neovascularization and granulation tissue formation. Ann Plast Surg 2004;52(5):519-521; discussion 522.

28. Hehenberger K, Heilborn JD, Brismar K, Hansson A. Inhibited proliferation of fibroblasts derived from chronic diabetic wounds and normal dermal fibroblasts treated with high glucose is associated with increased formation of l-lactate. Wound Repair Regen 1998;6(2):135-141.
29. Kim JH, Ruegger PR, Lebig EG, VanSchalkwyk S, Jeske DR, Hsiao A, et al. High Levels of Oxidative Stress Create a Microenvironment That Significantly Decreases the Diversity of the Microbiota in Diabetic Chronic Wounds and Promotes Biofilm Formation. Front Cell Infect Microbiol 2020;10:259.
30. Lou D, Luo Y, Pang Q, Tan WQ, Ma L. Gene-activated dermal equivalents to accelerate healing of diabetic chronic wounds by regulating inflammation and promoting angiogenesis. Bioact Mater 2020;5(3):667-679.
31. Nyambat B, Chen CH, Wong PC, Chiang CW, Satapathy MK, Chuang EY. Genipin-crosslinked adipose stem cell derived extracellular matrix-nano graphene oxide composite sponge for skin tissue engineering. J Mater Chem B 2018;6(6):979-990.
32. Lasocka I, Jastrzebska E, Szulc-Dabrowska L, Skibniewski M, Pasternak I, Kalbacova MH, et al. The effects of graphene and mesenchymal stem cells in cutaneous wound healing and their putative action mechanism. Int J Nanomedicine 2019;14:2281-2299.
33. Yu X, Luo Y, Chen G, Liu H, Tian N, Zen X, et al. Long noncoding RNA IGF2AS regulates high-glucose induced apoptosis in human retinal pigment epithelial cells. IUBMB Life 2019;71(10):1611-1618.
34. Li B, Zhou Y, Chen J, Wang T, Li Z, Fu Y, et al. Long non-coding RNA H19 contributes to wound healing of diabetic foot ulcer. J Mol Endocrinol 2020.
35. Horiguchi H, Kobune M, Kikuchi S, Yoshida M, Murata M, Murase K, et al. Extracellular vesicle miR-7977 is involved in hematopoietic dysfunction of mesenchymal stromal cells via poly(rC) binding protein 1 reduction in myeloid neoplasms. Haematologica 2016;101(4):437-447.
36. Chen L, Cao P, Huang C, Wu Q, Chen S, Chen F. Serum exosomal miR-7977 as a novel biomarker for lung adenocarcinoma. J Cell Biochem 2020;121(5-6):3382-3391.
37. Peng X, Ji C, Tan L, Lin S, Zhu Y, Long M, et al. Long non-coding RNA TNRC6C-AS1 promotes methylation of STK4 to inhibit thyroid carcinoma cell apoptosis and autophagy via Hippo signalling pathway. J Cell Mol Med 2020;24(1):304-316.
38. Guo F, Wang W, Song Y, Wu L, Wang J, Zhao Y, et al. LncRNA SNHG17 knockdown promotes Parkin-dependent mitophagy and reduces apoptosis of podocytes through Mst1. Cell Cycle 2020;19(16):1997-2006.

Tables

Table 1 The specific primers are provided

Name	Sequence
Linc00324	F-GACGAGCCCTCCTTTACCTT
	R-CTGGGGATTGAGATGCTTTCT
miR-7977	F-CGCGCGTTCCCAGCCAAC
	R-ATCCAGTGCAGGGTCCGAGG
miR-7977	5-GTCGTATCCAGTGCAGGGTCCGAGGTA TTCGCACTGGATA
RT primer:	CGACTGGTGC-3
GAPDH:	F-GAAGGTGAAGGTCGGAGTC, R-GAAGATGGTGATGGGATTTCC;
U6:	F-CTCGCTTCGGCAGCACA
	R-AACGCTTCACGAATTTGCGT;
U6 RT primer: 5-GGGCAGGAAGAGGGCCTA-3	
STK4:	F-AGAGTTGGACAGTGGAGGACCTTC
	R-GCCGCTTGGACTGGTACTTCTG

Figures

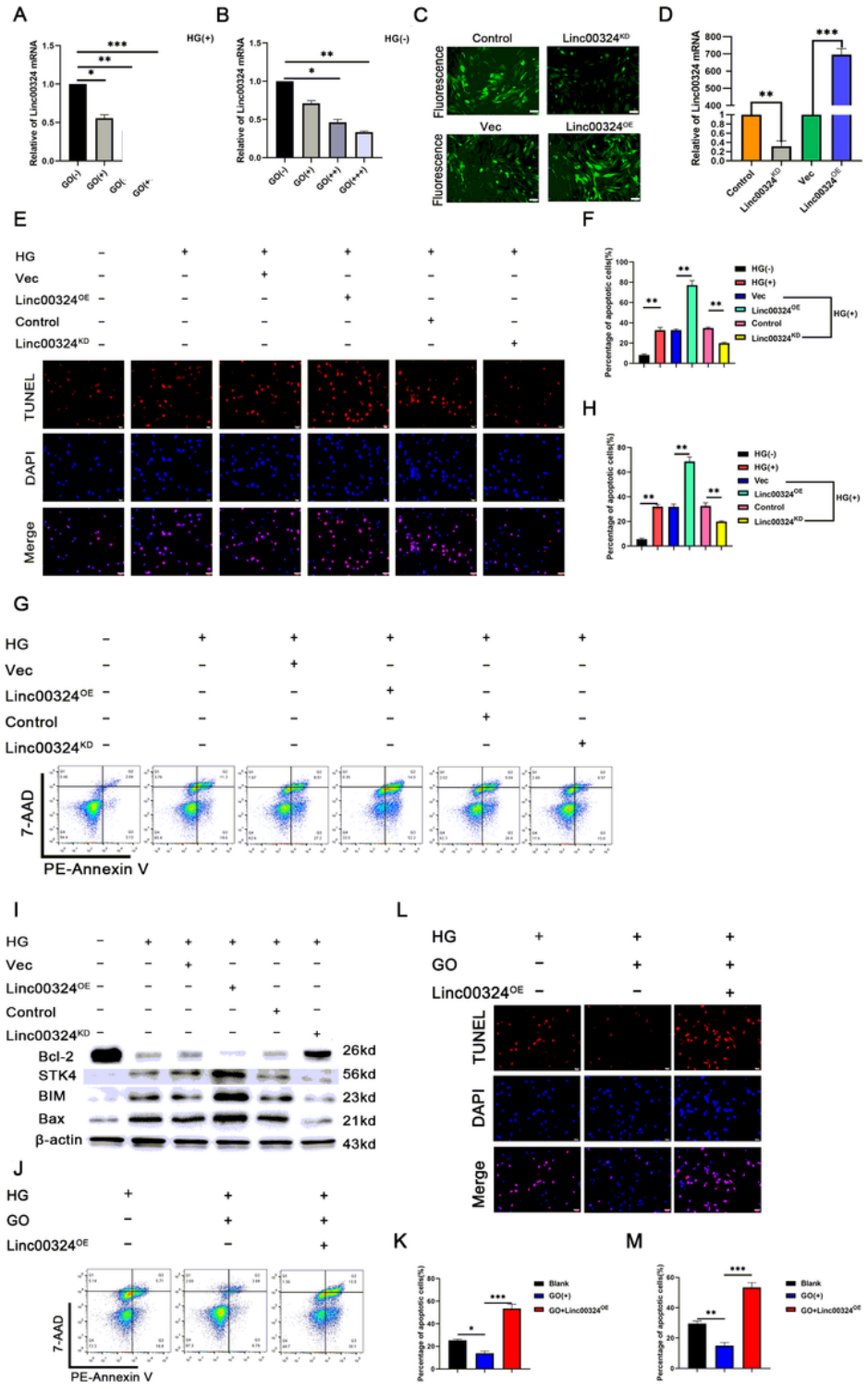

Figure 1

GO inhibited the expression of Linc00324 in Ad-MSCs. A. The expression of Linc00324 in Ad-MSCs after co-cultivation with GO was detected under high glucose environment. B. The expression of Linc00324 under normal environment. C, D. Fluorescence of down-regulated Linc00324 and overexpressing Linc00324, verify the effect of down-regulating Linc00324 and overexpressing Linc00324. Scale bar = 50 μm. E, F. Under high glucose environment, flow cytometry was used to detect Ad-MSCs apoptosis and

statistical analysis. G, H. The TUNEL assay detected cell apoptosis and statistical analysis.i.Western blot experiment detected apoptosis-related proteins BAX, BIM, STK4, BCL-2.Scale bar = 50 μm.Values shown are mean ± S.D. from three independent experiments, *p < 0.05, **p < 0.01, ***p < 0.001. Linc00324OE, overexpression of Linc00324; Linc00324KD, knockdown of Linc00324.

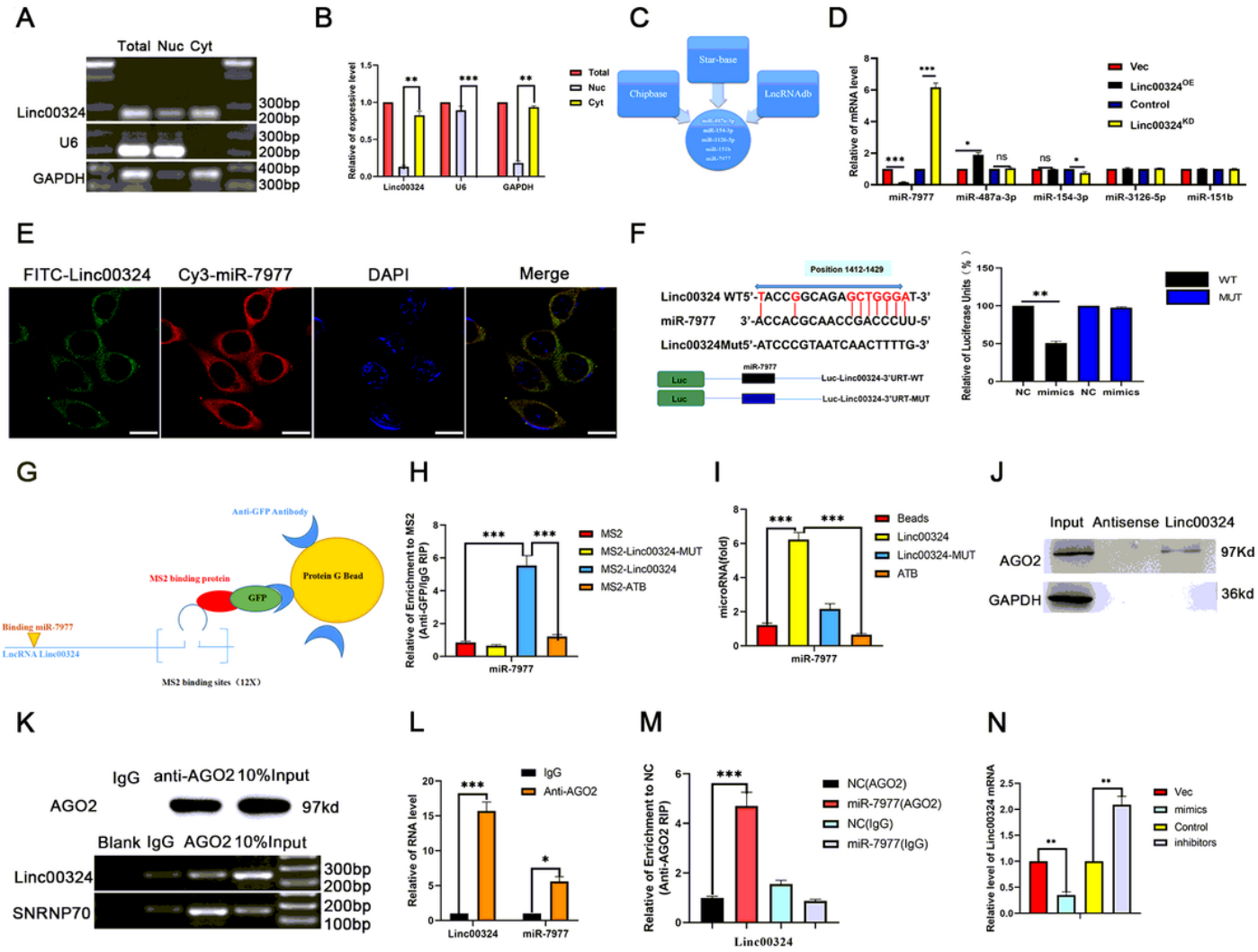

Figure 2

Linc00324 decoyed miR-7977 as a sponge RNA. A, B. Detected the expression of Linc00324, U6, GAPDH. C. microRNAs had binding relationship with Linc00324 in databases. D. Detected microRNAs by qRT-PCR. (E). FISH detections demonstrated them colocalized in cytoplasm. F. The wild-type Linc00324 bound miR-7977. G. The schematic diagram of GFP-MS2-RIP. H, I. Detected microRNAs associated with Linc00324. J. RNA pull-down assay shown the interaction between Linc00324 and AGO2. K. Results of the RIP assay. L. Levels of Linc00324, miR-7977 in the IgG group and the anti-AGO2 group. M. Anti-AGO2 RIP detected Linc00324 associated with AGO2. N. The mRNA of Linc00324 was detected. Scale bar = 20 μm.Values shown are mean ± S.D. from three independent experiments, *p < 0.05, **p < 0.01, ***p < 0.001.

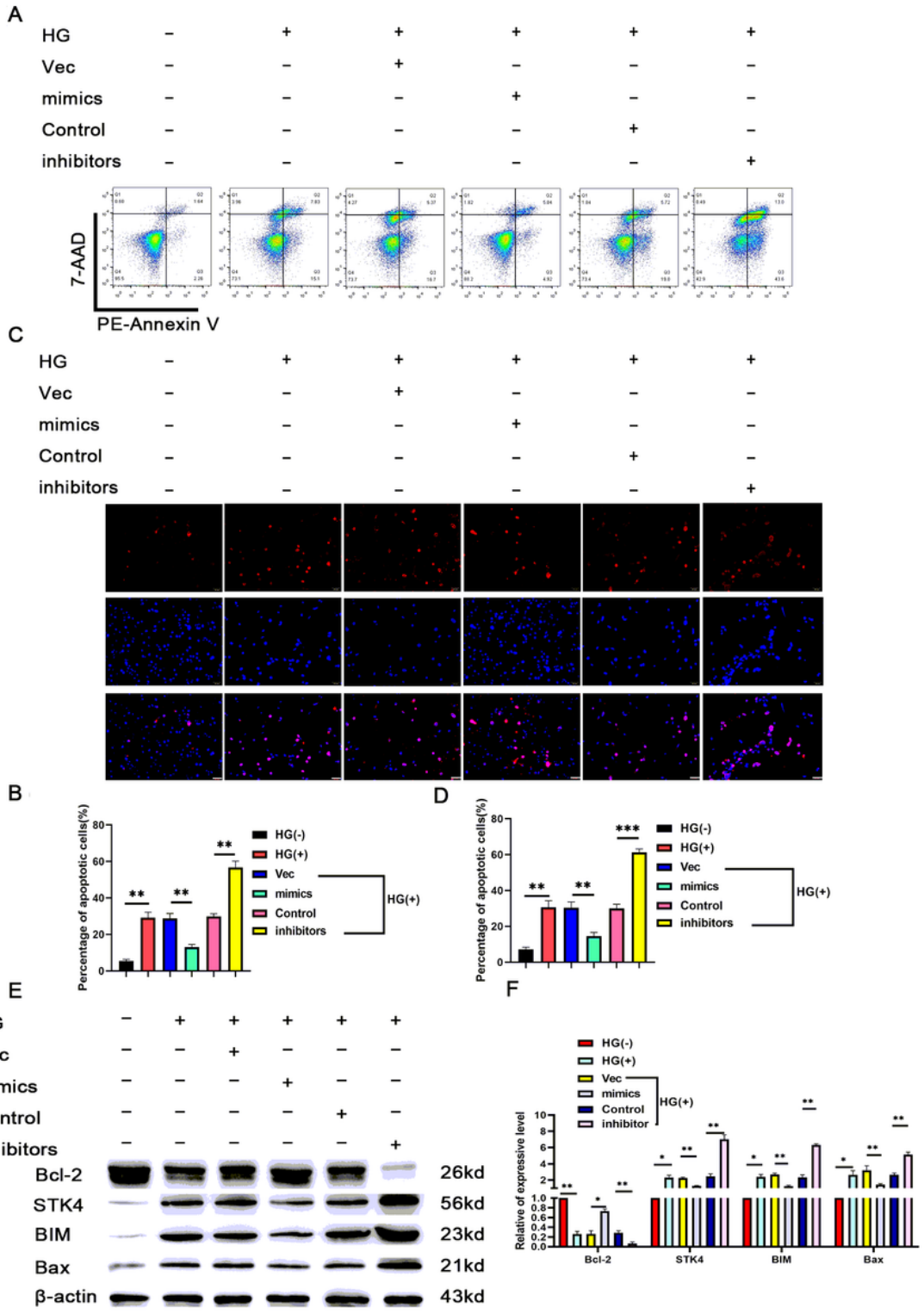

Figure 3

miR-7977 inhibited the apoptosis of Ad-MSCs. A, B. Flow cytometry was used to detect the apoptosis of Ad-MSCs and statistical analysis in a high glucose environment. C, D. TUNEL was used to detect the apoptosis of Ad-MSCs and statistical analysis under high glucose environment. E, F. Western blot experiment detected apoptosis-related proteins BAX, BIM, STK4, BCL-2 and statistical results. Scale bar =

50 μm.Values shown are mean ± S.D. from three independent experiments, *p < 0.05, **p < 0.01, ***p < 0.001.

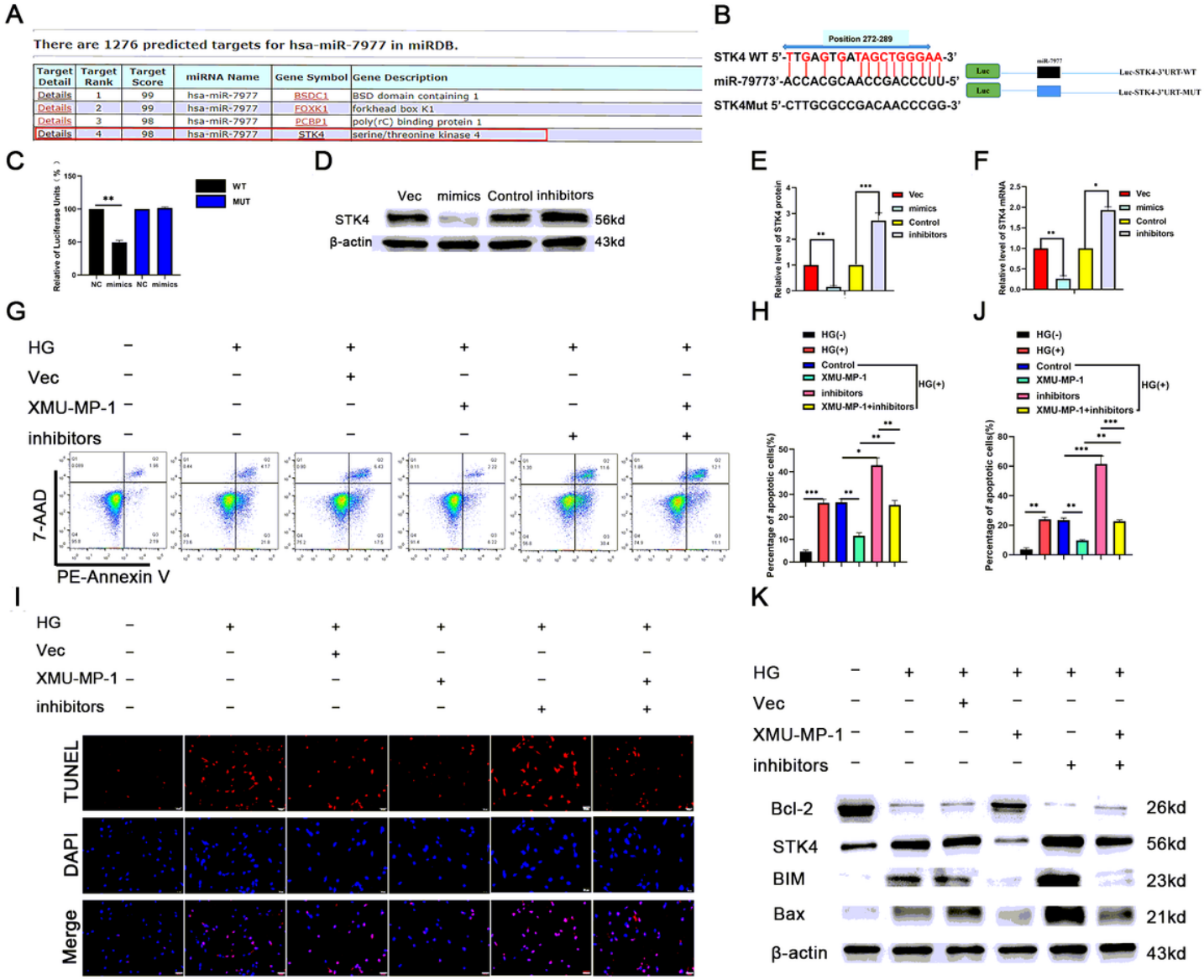

Figure 4

miR-7977 targeted STK4 to regulate apoptosis of Ad-MSCs. A. The predicted target STK4 of miR-7977 found in the miRDB database. B, C. miR-7977 bound STK4 for dual luciferase assays were shown. D-F. The protein and mRNA expression of STK4 was verified by Western blot and qRT-PCR after transferring miR-7977 mimics and inhibitors into Ad-MSCs. G, H. After transferring the miR-7977 inhibitors and adding STK4 inhibitor XMU-MP-1 to Ad-MSCs, the apoptosis of the cells was detected by flow cytometry. I, J. The apoptosis of the cells was detected by TUNEL assay. K. Western blot experiment detected apoptosis-related proteins BAX, BIM, STK4, BCL-2. Scale bar = 50 μm.Values shown are mean ± S.D. from three independent experiments, *p < 0.05, **p < 0.01, ***p < 0.001.

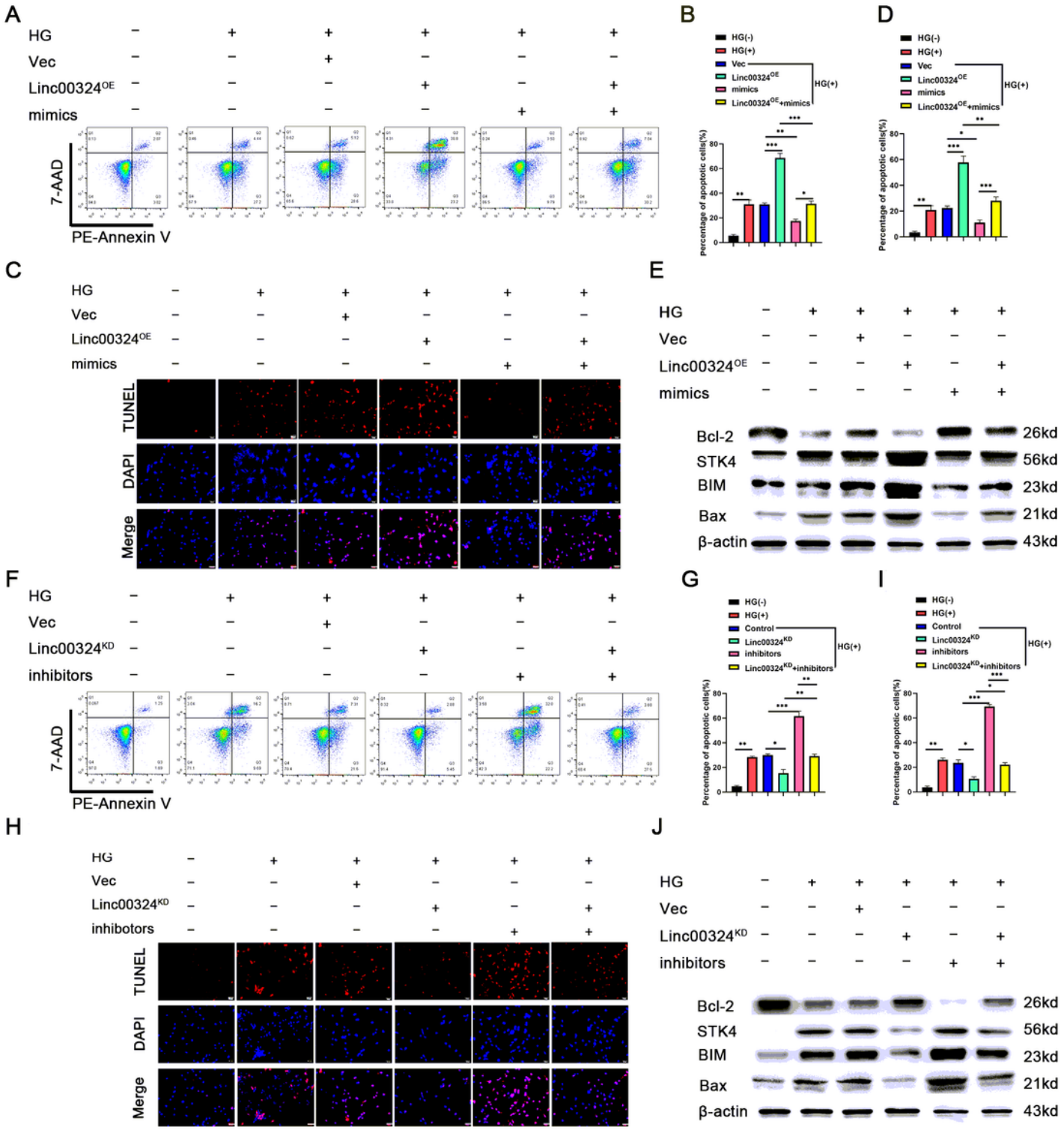

Figure 5

Linc00324 regulated the apoptosis of Ad-MSCs induced by high glucose through miR-7977/STK4. A, B. The miR-7977 mimics plasmid was transferred into Ad-MSCs and the apoptosis of Ad-MSCs was detected by flow cytometry and statistical analysis. C, D. TUNEL assay detected the apoptosis and statistical analysis. e. Western blot experiment detected proteins BAX, BIM, STK4, BCL-2. F, G. The miR-7977 inhibitors plasmid was transferred into Ad-MSCs and the apoptosis of Ad-MSCs was detected by

flow cytometry and statistical analysis. H, I. TUNEL assay detected the apoptosis and statistical analysis. J. Western blot experiment detected proteins BAX, BIM, STK4, BCL-2. Scale bar = 50 μm.Values shown are mean ± S.D. from three independent experiments, *p < 0.05, **p < 0.01, ***p < 0.001.

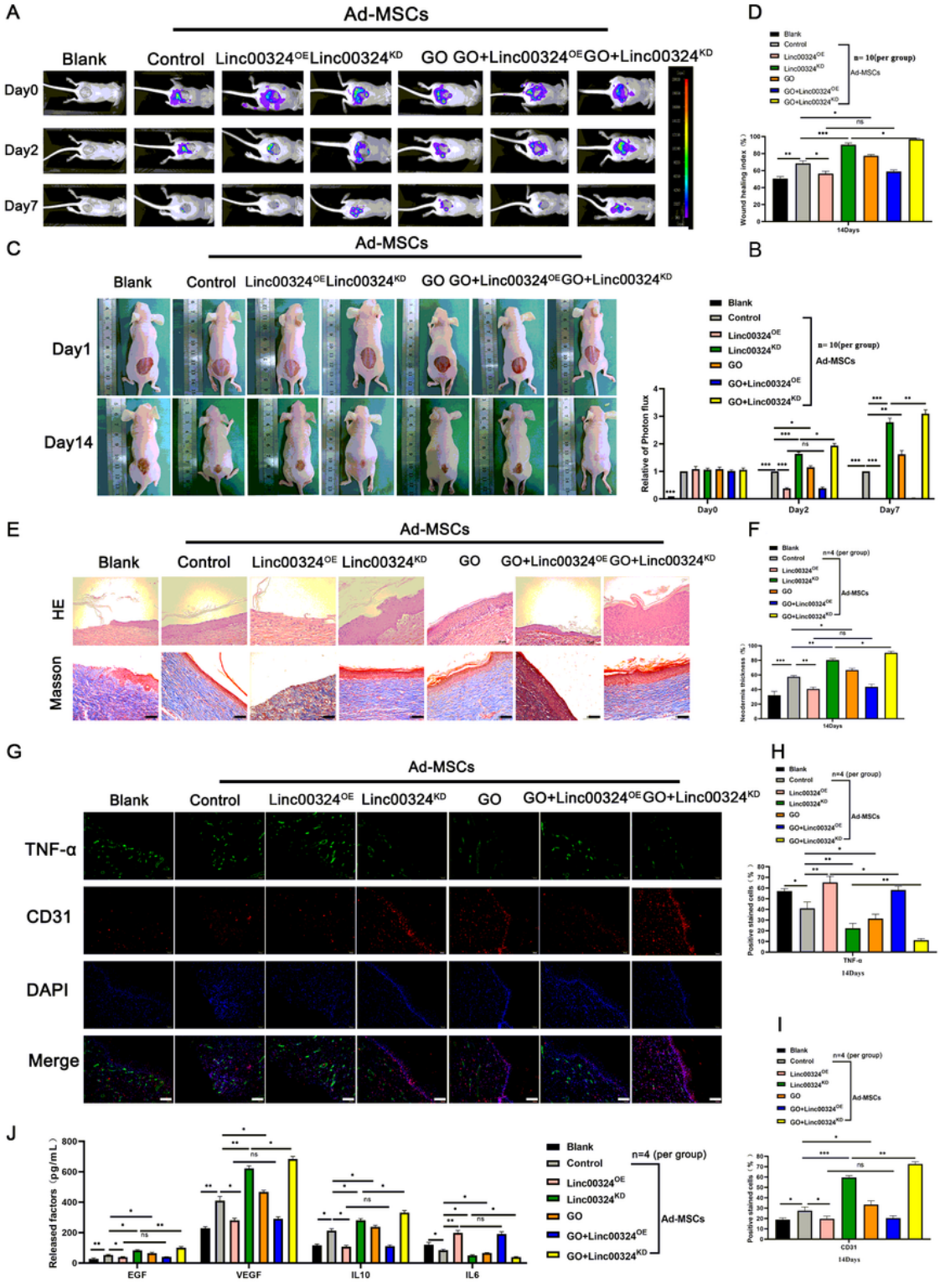

Figure 6

GO inhibited cell apoptosis and promoted wound healing in diabetic nude mice. A, B. Ad-MSCs stained with CM-Dil were injected into nude mice, analyzed the survival of Ad-MSCs. C, D. The healing situation

was observed 14 days after injection of different treatment fluids. E, F. On the 14th day, HE and Masson staining were performed to calculate the thickness of the newborn skin and analyze it statistically. Scale bar = 10 μm. G-I. The neonatal epidermis was taken for tissue fluorescence staining, including TNF-α (green), CD31 (red), and cell nucleus (blue). Scale bar = 50 μm. J. Elisa detected EGF, VEGF, IL10, and IL6. Values shown are mean ± S.D. from three independent experiments, *p < 0.05, **p < 0.01, ***p < 0.001.

Supplementary Files

This is a list of supplementary files associated with this preprint. Click to download.

- S1.tif
- S2.tif
- S3.tif
- S4.tif
- S5.tif
- S6.tif
- S7.tif
- S8.tif
- S9.tif
- SupplementaryText.doc